3-D Trajectory Optimization for Fixed-Wing UAV-Enabled Wireless Network

ALESSANDRO VISINTINI[1],
THARINDU D. PONNIMBADUGE PERERA [2], (Graduate Student Member, IEEE),
AND DUSHANTHA NALIN K. JAYAKODY [2,3], (Senior Member, IEEE)

[1]Industrial Engineering, Politecnico Di Milano, 20133 Milan, Italy
[2]School of Computer Science and Robotics, National Research Tomsk Polytechnic University, 634050 Tomsk, Russia
[3]Centre for Telecommunication Research, School of Engineering, Sri Lanka Technological Campus, Padukka 10500, Sri Lanka

Corresponding author: Dushantha Nalin K. Jayakody (nalin@tpu.ru)

ABSTRACT Unmanned aerial vehicles (UAVs) is a promising technology for the next-generation communication systems. In this article, a fixed-wing UAV is considered to enhance the connectivity for far-users at the coverage region of an overcrowded base station (BS). In particular, a three dimensions (3D) UAV trajectory is optimized to improve the overall energy efficiency of the communication system by considering the system throughput and the UAV's energy consumption for a given finite time horizon. The solutions for the proposed optimization problem are derived by applying Lagrangian optimization and using an algorithm based on successive convex iteration techniques. Numerical results demonstrate that by optimizing the UAV's trajectory in the 3D space, the proposed system design achieves significantly higher energy efficiency with the gain reaching up to 20 $bitsJ^{-1}$ compared to the 14 $bitsJ^{-1}$ maximum gain achieved by the 2D space trajectory. Further, results reveal that the proposed algorithm converge earlier in 3D space trajectory compare to the 2D space trajectory.

INDEX TERMS Energy efficiency, sequential convex optimization, trajectory optimization, UAV communication, 5G.

I. INTRODUCTION

Unmanned aerial vehicles (UAVs) has become an essential device in next generation communications with significant contribution made in open literature using it to fulfil high data demands of mobile users [1]. In fact, UAVs provide an efficient and dynamic distribution of radio resources [2]. High or low altitude UAV assisted communication systems are more cost-effective compared to tradition terrestrial communication systems. Apart from the cost-effectiveness, UAVs also provide more pros including on-demand communication links, flexible deployments with better controllability and better wireless channel conditions by having short line-of-sight (LoS) communication links. In addition, UAVs are expected to be widely used in future for wireless communication applications such as

The associate editor coordinating the review of this manuscript and approving it for publication was Emrecan Demirors .

surveillance and monitoring, aerial deliveries and remote sensing [3].

According to existing researches in open literature, UAVs have been mainly used in three categories for wireless communication networks. The first method is to use UAVs as a mobile base stations to assist seamy coverage areas in the existing terrestrial communication infrastructure [2], [4]. In this scenario, the UAV stays stationary above the service area for a given operational time until the batteries depleted. Second application of UAV is to use it as a relay node to assist reliable wireless connectivity between two or more communication nodes due to poor channel condition between them [1], [5]. The last category is to use UAVs to collect data from a wireless sensor networks for internet-of-things (IoT) applications, where UAVs have the role of collecting sensors' observations and hand them over to data sinks for further operations [3], [6].

The system performance of UAV assisted communication systems are fundamentally limited due its on-board energy constraint [1], [7]. Energy supply of the UAV is limited due to its mechanical structure and flying weight constraints. Thus, energy efficient design for UAV assisted communications is of paramount important to maintain the expected quality-of-service given by the traditional communication infrastructures. Energy efficient designs used for UAV assisted communication systems are slightly different compared to terrestrial communication systems [8]. Thus, energy efficient UAV enabled communication systems are widely investigated in open literature [1], [3], [5], [8]. In [1], the authors have proposed a new unified RF energy harvesting scheme to power of transmission capabilities of the UAV while optimizing the UAVs trajectory in three coordinates to minimize outage probability. In [3], the trajectory of UAV is optimized in three coordinates to maximize the minimum average data collection rate of all sensor nodes under the practical constraints of the communication systems. A new mobile relaying technique in [5] optimized a relay-UAV trajectory in 2D coordinates to maximize end-to-end throughput while selecting optimal power allocation in communication nodes to improve overall energy efficiency of the system. In [8], the authors study an energy-efficient UAV communication via 2D trajectory optimization considering propulsion energy consumption of the UAV. However, it is noteworthy that all the aforementioned research works considers only a single UAV in the respective communication systems [9].

In this article, we study an energy efficient design for UAV assisted communication, where multiple UAVs are used to assist the base station during cell overload scenario over a finite time horizon. In such a scenario, fixed-wing UAVs are used as relay nodes to assist information to the users who are in the boundary of the base station coverage area. The main objective is to optimize trajectory in three coordinate Cartesian plane to improve overall energy efficiency of the system during cell overload. Moreover, proposed energy-efficient trajectory design guarantees the balance between throughput maximization and UAV's energy consumption minimization in 3D trajectory unlike the conventional 2D trajectory design found in open literature. In particular, this is the first work in which the concept of energy efficiency have been proposed for multi UAV assisted overcrowded BS scenario using all the UAVs as relay nodes. Specifically, several solution are proposed and their results are compared within this article. The main contributions of this article are summarized as follows.

- We introduce multi-UAV assisted cooperative system model and derive the fixed wing UAV's energy consumption model in terms of UAV's propulsion energy. The propulsion energy consumption of the UAV is modelled as a function of UAV's acceleration and flying velocity as in [5]. It is also noteworthy that this energy consumption only works for fixed-wing UAVs, not for its counterpart rotary-wing UAVs. Then, we formulate

TABLE 1. List of abbreviations and acronyms.

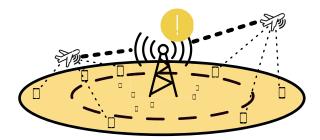|	
UAV	Unmanned Aerial Vehicle
GTs	Ground Terminals
SPC	Steady Plane Circular
5G	Fifth Generation
BS	Base Station
LoS	Line of Sight
ToF	Time of Flight
IoT	Internet of Things
KKT	Karush Kuhn Tucker
3D	Three dimensions
2D	Two dimensions
DF	Decode and forward
DOF	Degree of freedom
QoS	Quality of Service
QoE	Quality of Experience
CTM	Customizable

FIGURE 1. An illustration of the proposed system model. Multiple UAVs are serving the users located near the boundary of the overloaded base station's coverage area.

the optimization problem to maximize the energy efficiency of the proposed system.
- This article contains a complete description of closed-form solutions obtained analytically that solves the formulated problem. These solutions have been developed under strong assumptions upon the environment. Specifically, these theoretical solutions can be useful due to their low complexity, which makes them ideal for practical implementation.
- An algorithm based upon successive iteration technique is used for multi-UAV 3D trajectory optimization. Particularly, the convergence of the algorithm on a 3D scenario has been enquired. Due to the requirement of specific applications, the special case in which the final position and velocity are equal to the initial one is further investigated.
- Comparison between the 2D trajectory optimization algorithm presented in [6] and the aforementioned 3D multi-UAV optimization algorithm is provided, showing the difference in energy efficiency.

II. SYSTEM MODEL
As shown in Figure 2, it is considered a wireless communication system where multiple UAVs are employed as a relays to assist information transmission between a BS and GTs.
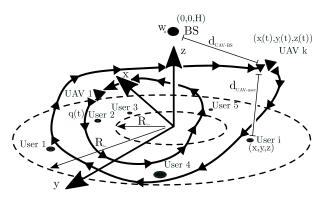
FIGURE 2. Sample UAVs' trajectory scheme of the system. It is shown the GTs (ground terminals) positions and the UAVs' trajectory.

The objective is to optimize the UAV's trajectory to maximize the energy efficiency in bits/Joule for a finite time horizon T, where the energy efficiency is defined as the ratio between the total information transmitted and the energy consumption over the mission duration T.

Without loss of generality, it is considered a three-dimensional (3D) Cartesian coordinate system such that the BS is located at $(0, 0, H)$ with a circular-shaped coverage area and the GTs are located in a circular crown centered on the origin, with the internal radius denoted as R_{int} and the external radius as R_{out}. K UAVs are capable of moving along x, y and z axis are considered. The trajectory of each UAV is denoted as: $q_k(t) = [x_k(t)\, y_k(t)\, z_k(t)]^T \in R^{3 \times 1}$, $0 \leq t \leq T$. Defining the position of the ith user assigned to the kth UAV as $w_{k,i} = [x_{k,i}\, y_{k,i}\, z_{k,i}]^T$, the coordinates of the $N_{u,k}$ GTs are assigned to the kth UAV are collected in K array as: $W_k = [w_{k,1}, \ldots, w_{k,i}, \ldots, w_{k,N_{u,k}}]$, being i the index used to identify the user. Thus, the time-varying distance between the kth UAV and the ith GT is:

$$d_{k,i}(t) = \sqrt{\left|\left|q_k(t) - w_{k,i}\right|\right|^2}, \quad 0 \leq t \leq T. \quad (1)$$

The BS position is defined as $w_a = [0, 0, H]$ and the distance between the BS and the kth UAV is given by:

$$d_k(t) = \sqrt{\left|\left|q_k(t) - w_a\right|\right|^2}, \quad 0 \leq t \leq T. \quad (2)$$

For ease of exposition, we assume that the communication links from the UAVs to the GTs and from UAVs to BS are experiencing LoS channel. Furthermore, the Doppler effect due to the UAV mobility is assumed to be perfectly compensated [8]. Thus, the time-varying channel follows the free-space path loss model. For the link k^{th} UAV-i^{th} GTs can be expressed as:

$$h_{k,i}(t) = \frac{\beta_0}{\left|\left|q_k(t) - w_{k,i}\right|\right|^2}, \quad 0 \leq t \leq T. \quad (3)$$

For the link BS-k^{th} UAV:

$$h_k(t) = \frac{\beta_0}{\left|\left|q_k(t) - w_a\right|\right|^2}, \quad 0 \leq t \leq T, \quad (4)$$

where β_0 denotes the channel power gain at the reference distance $d_0 = 1m$. Hypnotizing that each link is managed

by a different communication device, the instantaneous channel capacity in bits/second can be expressed for the link i^{th}GT-k^{th}UAV as:

$$
\begin{aligned}
r_{k,i}(t) &= B \log_2 \left(1 + \frac{P_{k,i}(t) h_{k,i}(t)}{\sigma_{k,i}^2}\right) \\
&= B \log_2 \left(1 + \frac{P_{k,i}(t) \beta_0}{\left|\left|q_k(t) - w_{k,i}\right|\right|^2 \sigma_{k,i}^2}\right), \quad 0 \leq t \leq T,
\end{aligned}
$$
$$(5)$$

where B denotes the bandwidth, $\sigma_{k,i}^2$ is the white Gaussian noise power. Transmission rate for the link between the kth UAV and the BS is:

$$r_k(t) = B \log_2 \left(1 + \frac{P_k(t) \beta_0}{\left|\left|q_k(t) - w_a\right|\right|^2 \sigma_k^2}\right), \quad 0 \leq t \leq T, \quad (6)$$

where σ_k^2 is the white Gaussian noise power. Assuming that $\sigma_k = \sigma_{k,i} = \sigma$, the total amount of information bits $I_{k,i}$ that can be transmitted from the k^{th}UAV to the ith GT over the duration T is a function of the kth UAV trajectory $q_k(t)$. It is expressed as:

$$I_{k,i} = \int_0^T B \log_2 \left(1 + \frac{P_{k,i}(t) \beta_0}{\left|\left|q_k(t) - w_{k,i}\right|\right|^2 \sigma^2}\right) dt. \quad (7)$$

The total amount of information bits I_k between the k^{th}UAV and the BS is expressed as:

$$I_k = \int_0^T B \log_2 \left(1 + \frac{P_k(t) \beta_0}{\left|\left|q_k(t) - w_a\right|\right|^2 \sigma^2}\right) dt. \quad (8)$$

In this work we are using a DF protocol, in order to have a reduced complexity in the optimization problem.

A. UAV ENERGY CONSUMPTION MODEL

The total energy consumption of the UAV includes two components called energy consumption for signal processing and propulsion energy. It is worth noting that, in practice, the communication-related energy is much smaller than the UAV's propulsion energy [8]. The total propulsion energy for the kth UAV is given below, as in [5].

$$
\begin{aligned}
E_k(q_k(t)) = \int_0^T \Bigg(& C_1 ||v_k||^3 + \frac{C_2}{||v_k||} \Bigg(1 \\
& + \frac{||a_k||^2 - \frac{(a_k^T v_k)^2}{||v_k||^2}}{g^2}\Bigg) + m a_k^T v_k \Bigg) dt, \quad (9)
\end{aligned}
$$

where $v_k = \dot{q}_k(t)$ and $a_k = \ddot{q}_k(t)$ denote the kth UAV velocity and acceleration vectors, C_1 and C_2 are two parameters related to the aircraft's weight, wing area and air density, g is the gravitational acceleration and m is the mass of the UAV including the payload [5]. Equation (9) can be re-written as:

$$
\begin{aligned}
E_k(q_k(t)) = \int_0^T \Bigg(& C_1 ||v_k||^3 + \frac{C_2}{||v_k||} \Bigg(1 \\
& + \frac{||a_k||^2 - \frac{(a_k^T v_k)^2}{||v_k||^2}}{g^2}\Bigg)\Bigg) dt + \Delta_k, \quad (10)
\end{aligned}
$$

where Δ_k is the term associated to the variation of kinetic energy.

B. ENERGY EFFICIENCY AND PROBLEM FORMALIZATION

The energy efficiency of the UAV communication system, is used in (10), (8) and (7) can be expressed as follows:

$$EE(q_k, v_k, a_k) = \frac{\sum_{k=1}^{K} \sum_{i=1}^{N_{u,k}} I_{k,i} + \sum_{k=1}^{K} I_k}{\sum_{k=1}^{K} E_k}. \tag{11}$$

The analysis perform in this work, considers the total information transmitted to the user plus the one transmitted to the BS at the numerator. This is mainly due to the fact that the UAV has an on-board memory, which is capable of properly allocating the information on the base of the available rate. The problem is:

$$\max_{q_k, v_k, a_k} EE(q_k, v_k, a_k) \tag{P0}$$

$$\text{subject to } ||v_k(t)|| < v_{max}, \quad \forall k, \tag{C0.1}$$

$$||v_k(t)|| > v_{min}, \quad \forall k, \tag{C0.2}$$

$$||a_k(t)|| < a_{max}, \quad \forall k, \tag{C0.3}$$

$$I_k > I_{a_{min}}, \quad \forall k, \tag{C0.4}$$

$$I_{k,i} > I_{i_{min}}, \quad \forall k, \tag{C0.5}$$

$$z_k(t) > h_{min}, \quad \forall k, i, \tag{C0.6}$$

$$\dot{z}_k(t) < v_{z,max}, \quad \forall k, i, \tag{C0.7}$$

$$||q_r(t) - q_s(t)|| > \hat{d}_{coll}, \quad \forall r, s, \ r \neq s, \tag{C0.8}$$

$$q_k(0) = \hat{q}_{0,k}, \tag{C0.9}$$

$$q_k(T) = \hat{q}_{0,k}, \tag{C0.10}$$

$$v_k(0) = \hat{v}_{0,k}, \tag{C0.11}$$

$$v_k(T) = \hat{v}_{0,k}. \tag{C0.12}$$

The problem (P0) represents the energy efficiency problem of the proposed system. It is defined as the ratio between the total number of information transmitted over the energy spent for the mission by all the UAVs. Constraint (C0.1) determines a maximum value to the norm of the velocity of the UAVs. Constraint (C0.2) and (C0.3) determine minimum and maximum values to the norm of the velocity of the UAVs, respectively. Constraint (C0.4) asserts a minimum value to the number of information in the link between the BS and the kth UAV. The minimum value to the number of information in the link between the ith user and the kth UAV is given by the constraint (C0.5). Constraint (C0.6) makes sure that UAV is always flying above the minimum height. Constraint (C0.7) asserts the maximum vertical velocity of the UAVs. The non-collision constraint denotes by (C0.8). Constraints relevant to initial position and final positions of the UAVs are denote by (C0.9) and (C0.10), respectively. The constraints over the initial and final velocity of the UAVs denote by (C0.11) and (C0.12), respectively. Considering the formulation of (12), it is straightforward to note that is complex to

TABLE 2. List of all the methodologies used to solve the problem (12).

Name	DOF	Problem	Section
Cone bounded trajectory optimization	1	(P1)	III
Three DOF bounded trajectory	3	(P2)	IV
Constraint and bounded three DOF trajectory	3	(P3)	V
Unbounded 3D trajectory	CTM	(P4)	VI
Unbounded 2D trajectory	CTM	(P6)	VII

solve for two reasons. First, (12) requires the optimization of the continuous function $q_k(t)$, its first order derivative given by the velocity $v_k(t)$ and its second order derivative given by the acceleration $a(t)$. This fact involves an infinite number of optimization variables. The second reason is that the energy efficiency is given by a fraction of two integrals, both lacking a closed-form expression. In the next section, this article solves the problem reducing the variables for each UAV.

III. CONE BOUNDED TRAJECTORY OPTIMIZATION

In order to obtain a mathematically tractable analysis for (12), in this section, we propose an energy-efficient design by assuming UAVs are following a simple circular trajectory centered at the BS as shown in Figure 3. Furthermore, a higher number of GTs are presented, lying on a circumference or radius $R_{mid} = (R_{ext} + R_{int})/2$. Thus, the UAV is practically communicating with an antenna of a circular shape, reducing the scenario to a 2D problem as shown in Figure 3. Furthermore, the transmission power is fixed, such that it is the similar for all the links ($P_{k,i} = P_k = P$) and $\gamma_0 = P\beta_0$ [8]. Thus, the energy efficiency defined in (11) reduces to a simpler closed-form expression (53) given in the Appendix A. Specifically, for steady plane circular (SPC) flight with constant speed of the kth UAV V_k and trajectory of radius $R_{trj,k}$, we have $||v_k(t)|| = V_k$, $a_k^T(t)v_k(t) = 0$ and $||a_k(t)|| = V_k^2/R_{trj,k} \ \forall t$. Furthermore, it is supposed that the trajectory circumference is owed by the cone having the BS as a vertex and owe the GTs circumference. Defining s as the distance between the trajectory plane and the BS as shown in Figure 4, $L = \sqrt{H^2 + R_{mid}^2}$, $\theta = \tan^{-1}(H/R_{mid})$, $R_{trj,k} = s_k \cos(\theta)$, and according to the derivations reported in the Appendix B, it is possible to re-write the equation of the UAVs energy consumption and the total number of information transmitted. Assuming a DF protocol, it is imposed that $r_{u,k} = r_{a,k}$. Thus, the energy efficiency is written as:

$$EE_I(s_k, V_k)$$

$$= \frac{\sum_{k=1}^{K} TB \log_2 \left(1 + \frac{\gamma_0}{s_k^2}\right) + \sum_{k=1}^{K} TB \log_2 \left(1 + \frac{\gamma_0}{(L-s_k)^2}\right)}{\sum_{k=1}^{K} T\left[\left(C_1 + \frac{C_2}{g^2 R_{trj,k}^2}\right) V_k^3 + \frac{C_2}{V_k}\right]}. \tag{12}$$
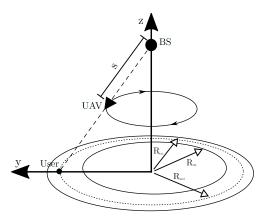
FIGURE 3. Scheme of cone constrained trajectory optimization for one UAV. In this scenario, the geometry is much simplified.
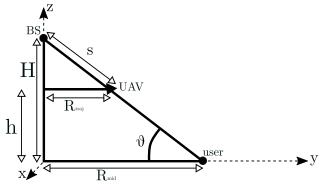

FIGURE 4. A trigonometrical representation of a cone constrained trajectory optimization for one UAV.

The corresponding problem can be formalized as:

$$\max_{V_k, s_k} EE_{probI}(V_k, s_k) \tag{P1}$$

$$\text{subject to } s_k < s_{max}, \tag{C1.1}$$

$$s_k > s_{min}, \tag{C1.2}$$

$$V_k < v_{max}, \tag{C1.3}$$

$$V_k > v_{min}, \tag{C1.4}$$

$$V_k^2 / R_{trj} < a_{max}, \tag{C1.5}$$

$$r_{u,k} = r_{a,k}. \tag{C1.6}$$

In order to solve (C1.1), it is written in the form of the Lagrangian $\mathcal{L}_I$ as:

$$\mathcal{L}_I(s_k, V_k, \lambda_k) = (C1.1) + \lambda_1(r_{u,1} - r_{a,1}) + \lambda_2(r_{u,2} - r_{a,2})$$
$$+ \ldots\ldots + \lambda_K(r_{u,K} - r_{a,K}). \tag{15}$$

Imposing $\partial\mathcal{L}_I / \partial\lambda_k = 0$, it is straightforward to find $s_k = L/2$. This being the only solution, it is can be considered as an optimal solution, which is denoted with s_k^* for each UAV. At this point, since the velocity V_k affects only the denominator of (C1.1), it is found that imposing $\partial\mathcal{L}_I / \partial V_k = 0$ and evaluating the second derivative of (53),

the optimal velocity V_k^* of every UAV can be found as:

$$V_k^* = V^* = \left(\frac{C_2}{3\left(\frac{C_2}{(gs_k^* \cos(\theta))^2} + C_1 \right)} \right)^{\frac{1}{4}}. \tag{16}$$

In the next section, we will solve the problem constraining the trajectory so that there are three variables for each UAV.

IV. THREE DOF BOUNDED TRAJECTORY

In order to obtain another mathematically tractable analysis, we refer to figure 5. Particularly, the UAVs circular trajectory is no more constrained to the aforementioned cone and the variables are the radius of each UAV R_k, the height of the trajectory plane h_k and the norm of the velocity V_k. The proof is provided in Appendix C. Since the total number of information transmitted and the energy consumed for the flight depends on each UAV, the optimization will be carried out considering a UAV. Consequently, the energy efficiency becomes:

$$EE_{II}(V, R, h) = \frac{I_a(R, h) + I_u(R, h)}{E(V, R)}. \tag{17}$$
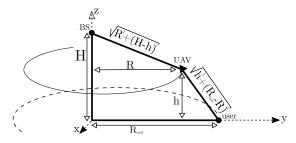

FIGURE 5. Scheme of three DOF and two DOF trajectory for one UAV. The variables are *R* (trajectory radius), *h* (trajectory plane height) and *V* (UAV velocity).

Therefore, the problem can be formalized as:

$$\max_{V, R, h} EE_{II}(V, R, h) \tag{P2}$$

$$\text{subject to } R < R_{max}, \tag{C2.1}$$

$$R > 0, \tag{C2.2}$$

$$h < h_{max}, \tag{C2.3}$$

$$h > h_{min}, \tag{C2.4}$$

$$V < v_{max}, \tag{C2.5}$$

$$V > v_{min}, \tag{C2.6}$$

$$V^2 / R < a_{max}, \tag{C2.7}$$

$$r_u = r_a. \tag{C2.8}$$

In order to solve (P2), it is written in the form of the Lagrangian $\mathcal{L}_{II}$ as:

$$\mathcal{L}_{II}(R, h, V, \lambda) = (P2) + \lambda(C2.8). \tag{19}$$

Imposing $\partial\mathcal{L}_{II} / \partial\lambda = 0$, it is found the following relation between the circumference radius R and the height h as:

$$R(h) = \frac{R_{mid}^2 + 2Hh - H^2}{2R_{mid}}, \tag{20}$$

where R_{mid} is defined as: $R_{mid} = (R_{ext} + R_{int})/2$. Joining this relation with constraint (C2.2), it is found a constraint over the height as:

$$h > \frac{H^2 - R_{mid}^2}{2H}. \tag{21}$$

Since the geometry imposes that $R_{mid} \gg H^2$ and recalling constraint given by Equation (C2.4), (21) is always satisfied if (C2.4) is satisfied. Substituting (20) in (19) evaluating $\partial \mathcal{L}_{II}/\partial V = 0$ and $\partial \mathcal{L}_{II}^2/\partial^2 V$, it is found that the optimal velocity expression V^* is the same of the one given by (16). At this point, the only variable to optimize is h and $\mathcal{L}_{II}(R, h, V, \lambda) \rightarrow \mathcal{L}_{II}(h)$. Substituting the optimal expression of the velocity V^* and $R(h)$, it is possible to obtain (19) as a single variable function:

$$\mathcal{L}_{II}(h) = \frac{2 \log_2 \left(1 + \frac{\gamma_0}{R(h)^2 + (H-h)^2} \right)}{\left(3^{-\frac{3}{4}} + 3^{\frac{1}{4}} \right) C_2^{\frac{3}{4}} \left(C_1 + \frac{C_2}{\left(gR(h) \right)^2} \right)^{\frac{1}{4}}}. \tag{22}$$

The next step is to understand the behavior of the function, in order to identify existence of maximum or stationary points. It holds that $\lim_{h \to \infty} \mathcal{L}_{II}(h) = 0$, $\mathcal{L}_{II}(h = \hat{h}_{min}) = \delta > 0$ and $\exists \mathcal{L}_{II}(h) \forall h > 0$. Therefore, a finite optimal solution h^* should exists and can be efficiently found analytically. Particularly, in the considered scenario, it holds that $h \ll R_{mid}$ and (20) becomes $R(h) \approx \frac{R_{mid}}{2}$. Applying this result into (22), it can be further simplified as:

$$\mathcal{L}_{II}(h) = \frac{2B \log_2 \left(1 + \frac{\gamma_0}{(R_{mid}/2)^2 + (H-h)^2} \right)}{\left(3^{-\frac{3}{4}} + 3^{\frac{1}{4}} \right) C_2^{\frac{3}{4}} \left(C_1 + \frac{C_2}{\left(gR_{mid}/2 \right)^2} \right)^{\frac{1}{4}}}. \tag{23}$$

Imposing $d\mathcal{L}_{II}(h)/dh = 0$, It is possible to determine optimal height as:

$$h^* = H/2. \tag{24}$$

In the next section we will address the problem based on the analysis of the current section, imposing the initial position to be equal to the final one.

V. CONSTRAINT AND BOUNDED THREE DOF TRAJECTORY
In this section, we refer again to Figure 5. The analysis is based on the one of the previous section. This time, it is added the coincidence of initial and final conditions such that the operational time T is the duration of one lap. Due to considerations similar to the one of the previous scenarios, the energy efficiency is solved for one UAV. Thus, the energy efficiency can be written as

$$EE_{III}(V, R, h) = \frac{I_a(R, h) + I_u(R, h)}{E(V, R)}, \tag{25}$$

where $I_a(R, h)$, $I_u(R, h)$ and $E(V, R)$ as defined in the previous section. We assume that in each operational time T, the UAV complete one cycle. Thus, the problem can be formulated as:

$$\max_{V,R,h} EE_{III}(V, R, h) \tag{P3}$$

$$(C2.1) - (C2.8),$$
$$V = \frac{2\pi R}{T}. \tag{C3.1}$$

Lagrangian optimization is used to solve (P3):

$$\mathcal{L}_{III}(R, h, V, \lambda_1, \lambda_2) = (P3) + \lambda_1(C2.8) + \lambda_2(C3.1). \tag{27}$$

It is found again the $\partial \mathcal{L}_{III}/\partial \lambda_1 = 0$ as related to (20). When $\partial \mathcal{L}_{III}/\partial \lambda_2 = 0$, it obtained (26). Consequently, the dependence of $\mathcal{L}_{III}$ over V and R is lost. By imposing the constraint (C2.5), (C2.6) and (C2.7), a conditions over h is derived and proof is presented in Appendix D. Consequently, in this scenario we optimize h and $\mathcal{L}_{III}(r, h, V, \lambda_1, \lambda_2) \rightarrow \mathcal{L}_{III}(h)$ and it holds that:

$$\mathcal{L}_{III}(h) = \frac{2 \log_2 \left(1 + \frac{\gamma_0}{R(h)^2 + (H-h)^2} \right)}{\left(C_1 + \frac{C_2}{g^2 R(h)^2} \right) \left(\frac{2\pi R(h)}{T} \right)^3 + \frac{C_2 T}{2\pi R(h)}}. \tag{28}$$

This function has the following properties: $\lim_{h \to \infty} \mathcal{L}_{III}(h) = 0$, $\mathcal{L}_{III}(h = \hat{h}_{min}) = \delta > 0$ and $\exists \mathcal{L}_{III}(h) \forall h > 0$. Note that the problem (12) is difficult to solve as the trajectory $q_k(t)$, the velocity $v_k(t)$ and acceleration $a_k(t)$ are time-continuous variables implying an infinite number of optimization variables [8]. Therefore, it is possible through Newton method to efficiently find an optimal value for the height h^*, which is presented in the section VIII.

VI. UNBOUNDED 3D TRAJECTORY
The problem (P0) has an objective function which lacks closed-form expression. To make the problem more tractable, we use the linear discrete state-space approximation to reformulate this optimization problem. The energy consumption of the UAV is upper bounded and can be expressed as given is [8]:

$$\int_0^T \left(C_1 ||v_k(t)||^3 + \frac{C_2}{||v_k(t)||} \right.$$
$$\times \left. \left(1 + \frac{||a_k(t)||^2 - \frac{(a_k(t)^T v_k(t))^2}{||v_k(t)||^2}}{g^2} \right) \right) dt <$$
$$< \int_0^T \left(C_1 ||v_k(t)||^3 + \frac{C_2}{||v_k(t)||} \left(1 + \frac{||a_k(t)||^2}{g^2} \right) \right) dt, \tag{29}$$

It is worth noting that the upper bound for the energy consumption equation is tight when the UAV trajectory is at a steady circular flight [8]. The term related to the kinetic energy Δ_k is null since the initial and final conditions are the same. The time horizon T is discretized into $N + 2$ equally spaced time slots with step δ_t. Since $v_k(t)$ and $a_k(t)$ are denote $\dot{q}_k(t)$ and $\ddot{q}_k(t)$, using the first- and second-order Taylor approximation, it can be written as:

$$v_k(t + \delta_t) \approx v_k(t) + a_k(t)\delta_t, \quad \forall t, \tag{30}$$
$$q_k(t + \delta_t) \approx q_k(t) + v_k(t)\delta_t + \frac{1}{2}a_k(t)\delta_t^2, \quad \forall t. \tag{31}$$

At this point it possible to state that $q[n] = q(n\delta_t)$, $v[n] = v(n\delta_t)$ and $a[n] = a(n\delta_t)$, for $n = 0, \ldots, N+1$. Then, we have

$$v_k[n + 1] = v_k[n] + a_k[n]\delta_t, \quad n = 0, \ldots, N, \tag{32}$$

$$q_k[n+1] = q_k[n] + v_k[n]\delta_t + \frac{1}{2}a_k[n]\delta_t^2, \quad n = 0, \ldots, N. \tag{33}$$

Again, the transmission power is here considered constant. Then the achievable rate can be written as

$$r_{k,i}[n] = B\log_2\left(1 + \frac{\gamma_0}{||q_k[n] - w_{k,i}||^2}\right), \tag{34}$$

$$r_k[n] = B\log_2\left(1 + \frac{\gamma_0}{||q_k[n] - w_a||^2}\right). \tag{35}$$

The lower bound of the energy efficiency can be written as:

$$EE_{3D}^{lb}(q_k[n], v_k[n], a_k[n])$$

$$= \frac{\sum_{k=1}^{K}\sum_{n=1}^{N}\sum_{i=1}^{N_{uk}} r_{k,i}[n] + \sum_{n=1}^{N}\sum_{k=1}^{K} r_k[n]}{\sum_{k=1}^{K}\sum_{n=1}^{N}\left(C_1||v_k[n]||^3 + \frac{C_2}{||v_k[n]||}\left(1 + \frac{||a_k[n]||^2}{g^2}\right)\right)}, \tag{36}$$

where $EE_{3D}^{lb} < EE_{3D}$. Thus, the problem can be re-written as:

$$\max_{q[n],v[n],a[n]} EE_{3D}^{lb}(q[n], v[n], a[n]), \tag{P4}$$

$$\text{subject to } ||v_k[n]|| < v_{max}, \quad n = 1, .., N, \tag{C4.1}$$

$$||a_k[n]|| > a_{max}, \quad n = 0, .., N, \tag{C4.2}$$

$$z_k[n] > \hat{h}_{min}, \quad \forall k, i, \quad n = 0, .., N, \tag{C4.3}$$

$$q_k[0] = \hat{q}_{0,k}, \tag{C4.4}$$

$$q_k[N+1] = \hat{q}_{0,k}, \tag{C4.5}$$

$$v_k[0] = \hat{v}_{0,k}, \tag{C4.6}$$

$$v_k[N+1] = \hat{v}_{0,k}, \tag{C4.7}$$

$$v_k[n+1] = v_k[n] + a_k[n]\delta_t, \quad n = 0, .., N, \tag{C4.8}$$

$$q_k[n+1] = q_k[n] + v_k[n]\delta_t$$
$$+ \frac{1}{2}a_k[n]\delta_t^2, \quad n = 0, .., N, \tag{C4.9}$$

$$||v_k[n]|| > v_{min}, \quad n = 1, .., N, \tag{C4.10}$$

$$||q_r[n] - q_s[n]|| > \hat{d}_{coll},$$
$$\forall r, s, \quad r \neq s, \tag{C4.11}$$

$$I_k > I_{a_{min}}, \quad \forall k, i, \tag{C4.12}$$

$$I_{k,i} > I_{i_{min}}, \quad \forall k, i. \tag{C4.13}$$

Note that constraints (C4.1)-(C4.9) are convex, whereas (C4.10)-(C4.13) are non-convex. To tackle (C4.10), we inserted the slack variable $\tau_k[n]$ and we update the denominator of (36) as follows [8]:

$$\sum_{n=1}^{N}\sum_{k=1}^{K}\left(C_1||v_k[n]||^3 + \frac{C_2}{\tau_k[n]}\left(1 + \frac{||a_k[n]||^2||v_k[n]||^2}{g^2}\right)\right)\delta_t. \tag{38}$$

(38) is concave according to [8], [10] and (C4.10) is substituted with:

$$\tau_k[n] > v_{min} \quad \forall n, \quad \forall k, \tag{39}$$

and

$$||v_k[n]||^2 > \tau_k[n]. \tag{40}$$

Approximating with a Taylor expansion, (40) at $||v_k^j[n]||^2$ can be written as:

$$||v_k^j[n]||^2 \geq ||v_k^j[n]||^2 + 2v_k^{j^T}[n](v_k[n] - v_k^j[n])$$
$$= \psi_k(v_k[n]) \geq \tau_k^2[n], \tag{41}$$

where j refers to the local point. The non-convexity of (C4.11) is managed considering its global lower bound found by its first order Taylor expansion centered at $q_r^j[n]$ and $q_s^j[n]$. Then, we obtain:

$$||q_r[n] - q_k[n]||^2 \geq -||q_r^j[n] - q_k^j[n]||^2$$
$$+ 2(q_r^j[n] - q_k^j[n])^T(q_r[n] - q_k[n]). \tag{42}$$

Therefore, the constraint can be re-written as:

$$d_{coll}^2 \leq -||q_r^j[n] - q_k^j[n]||^2$$
$$+ 2(q_r^j[n] - q_k^j[n])^T(q_r[n] - q_k[n])$$
$$= \Gamma(q_k), \quad \forall n, \; r > k. \tag{43}$$

Note that (43) is convex since it is linear with respect to $(q_r[n] - q_k[n])$ [11]. The last two non-convex constraints are (C4.12) and (C4.13). To manage those constraint, a convex lower bound for the local point $||q_k^j[n] - w_{i,k/a}||$ is given as [6]:

$$I_{i,k/a}^{lb} = B\sum_{n=1}^{N}\left[\alpha_j[n] - \beta_j[n]\left(||q_k[n]||^2 - ||q_k^j[n]||^2\right)\right]. \tag{44}$$

Therefore, $\alpha_j[n]$ and $\beta_j[n]$ can be written as:

$$\alpha_j[n] = \log_2\left(1 + \frac{\gamma_0}{||q_k^j[n] - w_{i,k/a}||^2}\right), \tag{45}$$

$$\beta_j[n] = \frac{(\log_2)e\gamma_0}{(\gamma_0 + ||q_k^j[n] - w_{i,k/a}||^2)(||q_k^j[n] - w_{i,k/a}||^2)}. \tag{46}$$

Note that this expression is convex with respect to $||q_{k,j}[n] - w_{i,k/a}||$ [6]. Consequently, this expression provides a lower bound also for the numerator of the energy efficiency. Thus, energy efficiency can be re-written as:

$$EE_{3D}^{lb,j}(q[n], v[n], a[n])$$

$$= \frac{\sum_{k=1}^{K}\sum_{n=1}^{N}\sum_{i=1}^{N_{uk}} I_{i,k}^{lb} + \sum_{n=1}^{N}\sum_{k=1}^{K} I_{a,k}^{lb}}{\sum_{k=1}^{K}\sum_{n=1}^{N}\left(C_1||v_k[n]||^3 + \frac{C_2}{||v_k[n]||}\left(1 + \frac{||a_k[n]||^2}{g^2}\right)\right)}. \tag{47}$$

For every local point $q_k^j[n]$, $v_k^j[n]$, $d_k^j[n]$, it is possible to reformulate the optimization problem (C4.1) as:

$$\max_{q_k^j[n], v_k^j[n], d_k^j[n]} EE_{3D}^{lb,j}(q_k^j[n], v_k^j[n], d_k^j[n]) \qquad (P5)$$

subject to (C4.1) − (C4.9).

$$\tau_k[n] > v_{min} \quad \forall n, \quad \forall k, \qquad (C5.1)$$

$$\psi_k(v_k[n]) \geq \tau_k[n], \qquad (C5.2)$$

$$d_{coll}^2 \leq \Gamma(q_k), \quad \forall n, \; r > k, \qquad (C5.3)$$

$$I_k^{lb} > I_{a_{min}}, \quad n = 0, .., N, \qquad (C5.4)$$

$$I_{k,i}^{lb} > I_{i_{min}}, \quad n = 0, .., N. \qquad (C5.5)$$

Based on what already discussed, it readily follows that the objective value of (P5) gives a lower bound to that of problem (P4). Furthermore, problem (P5) is a fractional maximization problem, with a concave numerator, a convex denominator and convex constraints [10], [12]. Thus, (P5) can be efficiently solved via the bisection method or the standard Dinkelbach's algorithm for fractional programming [13]. Therefore, the original non-convex problem (12) can be solved by iteratively optimizing (P5), as given in [5], with the local point updated in each iteration j. The proposed steps to obtained the optimal values are summarized in Algorithm 1. Once the all variables are collected in an optimization state X, it can be defined as:

$$X = \left[X_1, \ldots, X_k, \ldots, X_K \right], \qquad (49)$$

where X_k can be represented as:

$$X_k = \left[q_k[1], \ldots, q_k[n], \ldots, q_k[N], v_k[1], \right.$$
$$\left. \ldots, v_k[N], a_k[1], \ldots, a_k[N], \tau_k[1], \ldots, \tau_k[N] \right]. \qquad (50)$$

It is now possible to state the algorithm considering X as the unique variable, which is given in Algorithm 1.

Algorithm 1 Sequential Convex Optimization Algorithm

Step 1: Initialize the trajectory X_0, set $j = 1$;
Step 2: Solve (P5) and determine X_j^* at X_{j-1};
Step 3: **if** $\left\| X_j - X_{j-1} \right\| < \epsilon$, **stop**;
Step 4: Update the iteration $j \to j + 1$;
Step 5: Update the local point $X_j^* \to X_{j-1}$;
Step 6: Go to Step 2.

According the analytical analysis given up to this point, it possible to derive the series X_j, determined through Algorithm 1, which converges to a point satisfying the KKT conditions.[1] Optimal KKT conditions are given in Lemma VI.1.

Lemma 1: The energy efficiency lower bound $EE_{3D}^{lb,j,*}$ found at the jth iteration is monotonically non-decreasing, i.e. $EE_{3D}^{lb,j,*} \geq EE_{3D}^{lb,j-1,*} \; \forall \; j \geq 1$. Furthermore, the sequence

---

[1]The interested reader should refer to [6], [9], and [17].

$X_j^*, \; j = 0, 1, ..,$ *converges to a point fulfilling the KKT optimal conditions of the original non-convex problem* (C4.1).

The proof of lemma 1 can be given as in [14]. By making use of KKT Theorem at the local point X^j as the fact that the lower bounds $\psi(v_k[n]), \Gamma(q_k)$ and $r_{i,k}^{lb}$ have an identical gradient of the functions they underestimates. In the next section, another solution of the problem available in literature is presented. Specifically, it will be used as a benchmark to compare the results of this section.

VII. BENCHMARK: UNBOUNDED 2D TRAJECTORY

The 2D trajectory optimization is a topic already explored in the literature. Particularly, Unbounded 2D trajectory optimization can be considered as a sub case of section VI. The formulation of the problem does not change compared to the previous one. The only difference of the problem formulation of this section is that the height of the UAV is fixed. For the sake of brevity, the complete formulation is not presented here. Defining $q_k[n] = [x_k[n], y_k[n], K]$, being K a constant, the problem can be given as:

$$\max_{q_k[n], v_k[n], a_k[n]} EE_{2D}^{lb}(q_k[n], v_k[n], a_k[n]) \qquad (P6)$$

subject to (C4.1) − (C4.13).

The strategy adopted to find an optimal solution is given in [5], [8] and [6].

VIII. NUMERICAL RESULTS
A. ANALYTICAL RESULTS
In this section, results are provided to validate the proposed design. Unless otherwise stated, the results provided in this section is for when $K = 1$. The communication bandwidth is $B = 1MHz$ and the noise power spectrum density is assumed to be $N_0 = -170dBm/Hz$. Thus, the corresponding noise power is $\sigma^2 = N_0 B = -110dBm$. We assume that the UAV transmission power is $P = 10dBm$ (or $0.01W$) for the link toward every user, and the reference channel power gain is $\beta_0 = -50dB$. Furthermore, it is assumed that $C_1 = 9.26 \times 10^{-4}$ and $C_2 = 2250$, such that the UAV's minimum speed is $V_{min} = 8m/s$. The UAV's maximum speed is $V_{max} = 100m/s$ along $x \; y$ axis and whereas $V_{max} = 20 \; m/s$. The mass of the UAVs is of 4 Kg, $R_{int} = 2000m$, $R_{out} = 3000m$, $R_{mid} = 2500m$ and $H = 50m$. Finally, the minimum height for the UAV has been considered as $h_{min} = 10m$. In a real case scenario, with the parameters of the height and velocity chosen, it must be ensured that flying at the given altitudes and velocities adhering to the rules and regulation of the municipal area and the country. Specifically, these parameters are meant for low population density scenario. In particularly, in this section, results concerning the semi-analytical scenarios in section in III, IV and V are presented. The result of the analytical scenario III and IV are the same, which are obtained as $V^* = 29.9158m/s$, $h^* = 25m$ and $R^* = 1500m$. For the scenario presented in V it is possible to find through Newton method that $V^* = 9.4261m/s$, $h^* = 37.34m$ and

$R^* = 1502m$. For both scenarios, the value of the energy efficiency is much lower than 1. All these results are obtained considering $T = 1000s$. Similar to (51) and (C4.1), it is not possible to have a benchmark for (C1.1), (C2.1) and (26). In fact, they are bounded to the nature of the problem considered and therefore, difficult to compare with other solutions presented in literature. The best way to compare the results of (P1), (P2), (P3), (P4) and (P6) is considered to be the values of the energy efficiency, that are reported in Table 3.

TABLE 3. Results of the scenarios for all the results the operational time is $T = 1000\,s$.

Name	EE (bits/J)	Average v(m/s)	Average a(m/s^2)
Cone bounded trajectory optimization	0.0581	29.9158	0
Three DOF bounded trajectory	0.0581	29.9158	0
Constraint and bounded three DOF trajectory	0.0243	9.4261	0
Unbounded 3D trajectory	19.71	29.6524	0.4024
Unbounded 2D trajectory	14.33	28.8877	1.1609

B. RESULTS FOR (P4) AND (P6)

In this section, results of the algorithm 1 is presented. Concerning the unbounded 3D trajectory optimization, the number of UAV is $K = 3$. Considering the dimensions of the three UAVs used in the simulation, the probability of a collision is reasonably low [15]. Thus, the non-collision constraint (C5.3) has not been included. For simulations on larger number of UAVs, the inclusion of this constraint is highly recommended. The number of users considered is $N_u = 9$ and for the multi-UAV scenario, the number of users for each UAV is $N_{u,k} = 3$. It is let $q_1[0] = q_1[N] = [R_{mid}, 0, H/2]^T$ and $v_1[0] = v_1[N] = [0, 2\pi R_{mid}/T, 0]^T$. The other two UAVs have an initial condition equal in magnitude but rotated of 120° and 240°. The initial guess for the trajectory of each UAV X_0 is given as the circular steady plane trajectory, with a motion according to the initial conditions, making one turn in a period T. The step size have been considered $\delta_t = 10\,s$ and the operational time is $T = 1000s$. Concerning 2D unbounded trajectory optimization, it is considered $K = 1$ and $N_u = 9$. It is let $q[0] = q[N] = [R_{mid}, 0, H/2]^T$ and $v[0] = v[N] = [0, 2\pi R_{mid}/T, 0]^T$. The initial guess for the trajectory is given as the circular steady plane trajectory, with a motion according to the initial conditions, making one turn in a period T. The step size have been considered $\delta_t = 10\,s$ and the operational time is $T = 1000s$.

In Figure 6, the trajectories found solving (C4.1) through Algorithm 1 are given. It is noted that the shape of the trajectory of each UAV remains close to the circular one,
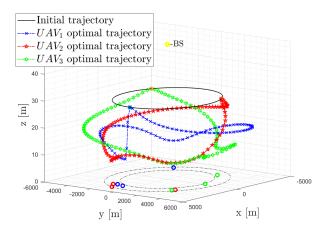

FIGURE 6. Optimized trajectory for unbounded 3D trajectory.

adjusting its height fulfilling the requirements over the minimum QoS and maximizing the overall energy efficiency. The highest point reached by the UAVs is the initial and final point, meaning that sensitivity analysis can be performed for a further energy efficiency increase. In Figure 7, it is possible to see how the third UAV spread his height.
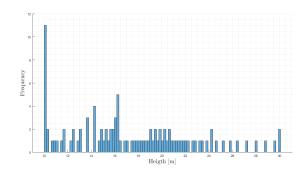

FIGURE 7. For the third UAV of the 3D optimized trajectory are classified the heights.

Next, we investigate the convergence for the 3D trajectory optimization Algorithm proposed in Figure 8. As expected, the energy efficiency increases at every iteration for (C4.1). Furthermore, for every iteration the convergence of Algorithm 1 follows that $EE_{3D} \geq EE_{3D}^{lb} \geq EE_{3D}^{lb,j}$. Moreover, it is possible to see that according to [14], EE_{3D}^{lb} and $EE_{3D}^{lb,j}$ are converging to a point fulfilling KKT conditions. Interestingly, the offset between EE_{3D} and EE_{3D}^{lb} is due to the fact that the upper bound for the energy consumption equation is tight when the UAV trajectory is a steady circular flight. Consequently, since the initial guess for the optimization is a circular steady flight, at the first iteration the difference is nonexistent and until the fourth iteration is negligible. The velocity of convergence is highly dependent on the time discretization step and number of users as well as their position. Considering (C4.1), with the similar number of users and the same discretization step, the convergence is obtained between 5th and 10th iterations. It has been observed
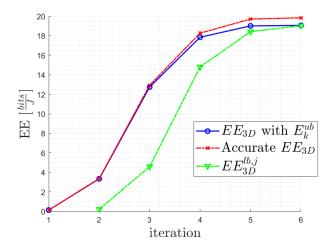
FIGURE 8. Convergence of Algorithm 1 applied to (C4.1). The Accurate EE_{3D} refers to the energy efficiency of (12). EE_{3D} with E_k^{ub} refers to (36) and $EE_{3D}^{lb,j}$ refers to the energy efficiency of (C5.1). All the values are computed using the trajectory at each iteration.
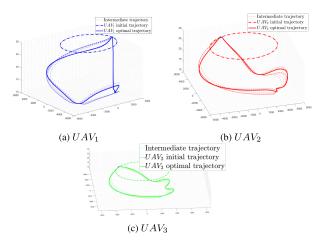

FIGURE 10. Convergence of Algorithm 1 applied to (51). The Accurate EE_{2D} refers to the energy efficiency of (12). It is also reported the EE_{2D} with E_k^{ub}. $EE_{2D}^{lb,j}$ refers to the energy efficiency of (51). All the values are computed using the trajectory at each iteration.

FIGURE 9. 3D Trajectory Evolution for the trajectories shown in Figure 6.

FIGURE 11. Optimized trajectory for unbounded 2D trajectory.

that if all the users assigned to a specific UAV are close to each other, the convergence is getting slower.

Unbounded 2D optimal trajectory results are shown in Figure 11. Interestingly, the UAV passes exactly over the users, in order to maximize the energy efficiency in that point since the distance is minimized and the rate is maximized. Between the users, the UAV minimizes the energy consumption maximizing through low energy maneuvers, represented by the protrusion of the trajectory.

Next, we investigate the convergence behavior of the unbounded 2D optimal trajectory in Figure 10. Again, we can see that the behavior of the energy efficiency for (51) solved by Algorithm 1 reflects the theory. Similar to Figure 8, at every iteration it holds that $EE_{2D} \geq EE_{2D}^{lb} \geq EE_{2D}^{lb,j}$, with EE_{2D}^{lb} and $EE_{2D}^{lb,j}$ converging to a point fulfilling KKT conditions. Also in this case, The offset between EE_{2D} and EE_{2D}^{lb} is due to the tight upper bound for the energy consumption in case of steady circular flight as in the initial condition. Interestingly, we note the superiority in terms of
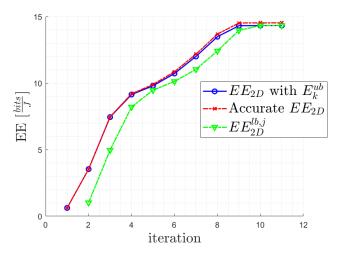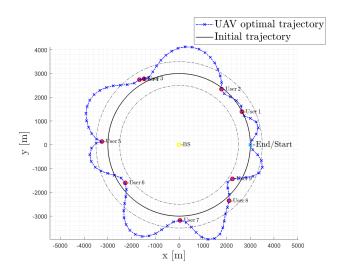
energy efficiency value of the 3D multiple UAV trajectory optimization with respect to the 2D single UAV trajectory optimization. Specifically, this superiority can be seen from the higher values of the energy efficiency obtained for the same number of users. In Figure 12, it is possible to see how the behavior of $||v_k||$ and $||a_k||$ of each UAV related to trajectories presented in Figure 6. Interestingly, $||v_k||$ remains constant around $30m/s$, meaning that an optimal velocity that maximizes the energy efficiency is found by the algorithm and the peaks of the acceleration are due to the users distribution. Finally, the evolution of the trajectories through the iterations for unbounded 3D trajectory optimization is shown in Figure 9. As expected, it can seen that in the 3D case the more the iterations are augmenting, the less the trajectory is circular, justifying the offset between EE_{3D} and $EE_{3D}^{lb,j}$ of Figure 8. Both the 3D and the 2D trajectory optimization simulations are made on a scenario with the same number
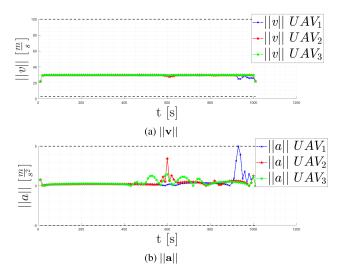
FIGURE 12. UAVs speed (a) and acceleration (b) according to the trajectories shown in Figure 6.

of users. Comparing the values of the energy efficiency it is possible to see the that the 3D multi UAV trajectory optimization provides a result superior with respect to the 2D single UAV. Unbounded 2D trajectory optimization have a slower convergence with respect to unbounded 3D trajectory optimization. This is mainly due to the fact that in the first case the UAV is just one and it has to serve all the users, whereas in the second case each UAV have to serve one third of the users within the communication network.

IX. CONCLUSION

This article studies the multiple 3D energy-efficient fixed-wing UAV relaying via trajectory optimization considering the propulsion energy consumption of the UAV. A mathematical formulation for the considered model is provided. Solution of the problem of increasing complexity are furnished. First, a scenario in which the solution is constrained to a 3D surface is considered with a possibility of deriving a closed-form solution. Next. a scenario with the UAV's trajectory supposed to be circular is considered in which radius, height and velocity are optimized allowing the formulation of two semi-analytical solutions. Finally, an efficient algorithm is used to maximize the energy efficiency based on linear state-space approximation and sequential convex optimization techniques. Numerical results show a significant increase of the energy efficiency with respect to the analytical and semi-analytical solutions proposed. Furthermore, numerical results depicted that the despite the numerical algorithm allow considering more constraints, it is computationally challenging for an UAV implementation. Finally, it was shown the superiority of the 3D multiple UAV trajectory optimization with respect to the 2D single UAV trajectory optimization.

APPENDIX A

Here it is demonstrated that:

$$I_{k,i}(q_{k,j}[n]) \geq I_{k,i}^{lb}(q_{k,j}[n]), \quad \forall q_{k,j}[n]. \quad (52)$$

Consider $h(z) = \log_2(1 + \gamma_0/(A + z))$, for $\gamma_0 \geq 0$ and A. It is possible to show that is convex for $A + z \geq 0$. Using the property of first-order Taylor expansion of a convex function as a global underestimator, for any given z_0, holds that $h(z) \geq h(z_0) + h'(z_0)(z - z_0)$, $\forall z$. Substituting $A = ||q_k[n] - w_{i,k}||^2$ and $z = ||q_k[n] - w_{i,k}||^2 - ||q_{k,j}[n] - w_{i,k}||^2$, it is readily follows the inequality just demonstrated. Furthermore, the two gradients of both the expression gradients are equal for $q_{k,j} = q_k$. The same holds for w_a.

APPENDIX B

Here are reported the derivations to get to the energy efficiency definition of the Cone bounded trajectory optimization. Defining s as the distance between the trajectory plane and the BS as shown in Figure 4 $L = \sqrt{H^2 + R_{mid}^2}$, $\theta = \tan^{-1}(H/R_{mid})$ and $R_{trj,k} = s_k \cos(\theta)$, (9) reduces to:

$$E(V_k, s_k) = \sum_{k=1}^{K} T\left[\left(C_1 + \frac{C_2}{g^2(s_k \cos(\theta))^2}\right)V_k^3 + \frac{C_2}{V_k}\right]. \quad (53)$$

Consequently, the information sent on the user circumference link I_u and the information sent on the BS link I_a becomes, respectively:

$$I_u = \sum_{k=1}^{K} TI_{u,k} = \sum_{k=1}^{K} TB \log_2\left(1 + \frac{\gamma_0}{(L - s_k)^2}\right), \quad (54)$$

$$I_a = \sum_{k=1}^{K} TI_{a,k} = \sum_{k=1}^{K} TB \log_2\left(1 + \frac{\gamma_0}{s_k^2}\right). \quad (55)$$

APPENDIX C

Here are reported (9) as well as I_u and I_a re-written according to the hypotheses presented in section IV.

$$E(V_k, R_k) = \sum_{k=1}^{K} T\left[\left(C_1 + \frac{C_2}{g^2 R_k^2}\right)V_k^3 + \frac{C_2}{V_k}\right]. \quad (56)$$

Similarly, I_u and I_a becomes:

$$I_a(R_k, h_k) = \sum_{k=1}^{K} TB \log_2\left(1 + \frac{\gamma_0}{R_k^2 + (H - h_k)^2}\right), \quad (57)$$

$$I_u(R_k, h_k) = \sum_{k=1}^{K} TB \log_2\left(1 + \frac{\gamma_0}{(R_{mid} - R_k)^2 + h_k^2}\right). \quad (58)$$

APPENDIX D

According to the hypotheses presented in section V, from (27) it is possible to identify the following condition over h:

$$\left(\frac{V_{min}T}{\pi}R_{mid} - R_{mid}^2 + H^2\right)\frac{1}{2H} < h \quad (59)$$

$$< \min\left\{\left(\frac{V_{max}T}{\pi}R_{mid} - R_{mid}^2 + H^2\right)\frac{1}{2H}, \quad (60)\right.$$

$$\left.\left(\frac{a_{max}T^2}{2\pi}R_{mid} + H^2 - R_{mid}^2\right)\frac{1}{2H}\right\}. \quad (61)$$

REFERENCES

[1] D. N. K. Jayakody, T. D. P. Perera, A. Ghrayeb, and M. O. Hasna, "Self-energized UAV-assisted scheme for cooperative wireless relay networks," *IEEE Trans. Veh. Technol.*, vol. 69, no. 1, pp. 578–592, Jan. 2020.

[2] N. Sharma, M. Magarini, D. N. K. Jayakody, V. Sharma, and J. Li, "On-demand ultra-dense cloud drone networks: Opportunities, challenges and benefits," *IEEE Commun. Mag.*, vol. 56, no. 8, pp. 85–91, Aug. 2018.

[3] C. You and R. Zhang, "3D trajectory optimization in rician fading for UAV-enabled data harvesting," *IEEE Trans. Wireless Commun.*, vol. 18, no. 6, pp. 3192–3207, Jun. 2019.

[4] A. Al-Hourani, S. Kandeepan, and S. Lardner, "Optimal LAP altitude for maximum coverage," *IEEE Wireless Commun. Lett.*, vol. 3, no. 6, pp. 569–572, Dec. 2014.

[5] Y. Zeng, R. Zhang, and T. J. Lim, "Throughput maximization for UAV-enabled mobile relaying systems," *IEEE Trans. Commun.*, vol. 64, no. 12, pp. 4983–4996, Dec. 2016.

[6] Y. Xu, L. Xiao, D. Yang, L. Cuthbert, and Y. Wang, "Energy-efficient UAV communication with multiple GTs based on trajectory optimization," *Mobile Inf. Syst.*, vol. 2018, pp. 1–10, Apr. 2018.

[7] Y. Huo, X. Dong, T. Lu, W. Xu, and M. Yuen, "Distributed and multilayer UAV networks for next-generation wireless communication and power transfer: A feasibility study," *IEEE Internet Things J.*, vol. 6, no. 4, pp. 7103–7115, Aug. 2019.

[8] Y. Zeng and R. Zhang, "Energy-efficient UAV communication with trajectory optimization," *IEEE Trans. Wireless Commun.*, vol. 16, no. 6, pp. 3747–3760, Jun. 2017.

[9] A. Visintini, T. Perera, D. N. Jayakody, and I. Pitas, "UAV trajectory optimization in modern communication systems: Advances and challenges," in *Proc. IEEE Int. Forum Strategic Technol. (IFOST)*, Tomsk, Russia, Oct. 2019.

[10] S. Boyd and L. Vandenberghe, *Convex Optimization*. Cambridge, U.K.: Cambridge Univ. Press, 2004.

[11] G. Zhang, H. Yan, Y. Zeng, M. Cui, and Y. Liu, "Trajectory optimization and power allocation for multi-hop UAV relaying communications," *IEEE Access*, vol. 6, pp. 48566–48576, 2018.

[12] *Introduction to Convex Constrained Optimization, Massachusetts Institute of Technology*. Accessed: Nov. 14, 2019. [Online]. Available: https://ocw.mit.edu/courses/sloan-school-of-management/15-094j-system%s-optimization-models-and-computation-sma-5223-spring-2004/lecture-notes/conve% x_opt_art.pdf

[13] J.-P. Crouzeix and J. A. Ferland, *Algorithms for Generalized Fractional Programming*. Cambridge, U.K.: Springer, 1991.

[14] A. Zappone, E. Björnson, L. Sanguinetti, and E. Jorswieck, "Achieving global optimality for energy efficiency maximization in wireless networks," *ArXiv*, vol. abs/1602.02923, 2016.

[15] Joint Authorities for Rulemaking on Unmanned Systems(JARUS). (2020). *JARUS, Guidelines on Specific Operations Risk Assessment*. [Online]. Available: http://jarus-rpas.org/

THARINDU D. PONNIMBADUGE PERERA (Graduate Student Member, IEEE) received the B.Sc. degree (Hons.) in software engineering and the M.Sc. degree from the Department of Computing, Faculty of ACES, Sheffield Hallam University, U.K. He is currently pursuing the Ph.D. degree in computer science and wireless communications with the Infocomm Laboratory, School of Computer Science and Robotics, National Research Tomsk Polytechnic University, Russia.

He has received a full-time scholarship from the Ministry of Education, Russian Federation, for his Ph.D. studies. He is currently a Research Engineer with the Department of IT, School of Computer Science and Robotics, National Research Tomsk Polytechnic University. His research interests include simultaneous wireless information and power transfer, interference exploitation in RF energy harvesting, and unmanned aerial vehicle-assisted communication.

DUSHANTHA NALIN K. JAYAKODY (Senior Member, IEEE) received the Ph.D. degree in electronics, electrical, and communications engineering from the University College Dublin, Ireland, in 2013. From 2014 to 2016, he was a Post-Doctoral Research Fellow with the Institute of Computer science, University of Tartu, Estonia, and the Department of Informatics, University of Bergen, Norway. Since 2016, he has been a Professor with the School of Computer Science and Robotics, National Research Tomsk Polytechnic University, Russia. Since 2019, he has been serving as the Dean with the School of Postgraduate and Research, Sri Lanka Technological Campus (SLTC), Padukka, Sri Lanka, where he is also the Founding Director of the Centre of Telecommunication Research. He has received the Best Paper Award from the IEEE International Conference on Communication, Management and Information Technology in 2017 and the International Conference on Emerging Technologies of Information and Communications, Bhutan, in 2019. In 2019, he received the Education Leadership Award from the World Academic Congress in 2019. In 2017 and 2018, he received the Outstanding Faculty Award from National Research Tomsk Polytechnic University, Russia. He also received Distinguished Researcher Award in wireless communications in Chennai, India, in 2019. He has authored or coauthored over 140 international peer-reviewed journal and conference articles and books. His research interests include PHY and NET layer prospective of 5G communications technologies, such as NOMA for 5G, cooperative wireless communications, device-to-device communications, LDPC codes, and unmanned aerial vehicle. He has organized or co-organized more than 20 workshops and special sessions of various IEEE conferences. He also served as the Chair, the Session Chair, or a Technical Program Committee Member for various international conferences, such as the IEEE PIMRC 2013–2019, the IEEE WCNC 2014–2018, and the IEEE VTC 2015–2018. He currently serves as an Area Editor for the *Elsevier Physical Communications Journal*, *MDPI Information Journal*, and the *Wiley Internet of Technology Letters*. He also serves as a reviewer for various IEEE TRANSACTIONS and other journals.

ALESSANDRO VISINTINI received the B.Sc. degree in aerospace engineering and the M.Sc. degree in space engineering from the Politecnico di Milano, Italy, in 2017 and 2020, respectively. In 2019, he was a Visiting Research Intern with the Infocomm Laboratory, School of Computer Science and Robotics, National Research Tomsk Polytechnic University, Russia. His research interests include unmanned aerial vehicle communication and trajectory optimization, and guidance, navigation, and control for aerospace and space vehicles.